Line shape, frequency shift, Rabi splitting, and two-photon resonances in four-level double-resonance spectroscopy with closely spaced intermediate levels

Swapan Mandal and Pradip N. Ghosh*
Department of Physics, University of Calcutta, 92, A.P.C. Road, Calcutta 700009, India
(Received 6 October 1992)

The interaction of a four-level atomic system with two electromagnetic radiations has been studied. The two intermediate levels are closely spaced such that a single radiation frequency can induce transitions from the ground state to both of them. In a cascade-type double resonance, the pump electric-field amplitude is much stronger than the amplitude of the signal field, which can induce transitions from both of the intermediate levels to the upper state. The 15 optical Bloch equations obtained from the Liouville equations are solved analytically to obtain the Doppler-free signal line shape. The computed signals, exhibiting two Lorentzian line profiles, are presented for different pump frequencies. In addition to these one-photon transitions, we obtain a weak two-photon resonance peak. The two-photon resonance becomes weaker when the detuning of the pump frequency from a resonance frequency is increased. When the pump frequency Ω_p is intermediate between the pump resonance frequencies ω_1 and ω_2, the two-photon resonance is very weak and almost vanishes when $\Omega_p=(\omega_1+\omega_2)/2$. When the pump frequency is on resonance with one of the transition frequencies, the Rabi splitting of the signal shows asymmetry because of the presence of a close-lying transition which is pumped off resonance. The intensity-dependent shifts of the transitions are such that they repel each other more and more as the intensity of the pump field is increased. These shifts arise from the nonresonant interaction between the atom and the field.

PACS number(s): 32.70.Jz, 33.70.Jg

I. INTRODUCTION

Double-resonance techniques are widely used in atomic and molecular spectroscopy. The pump field saturates one of the allowed transitions with the help of a strong external radiation field. The signal field is relatively weaker compared to the pump field. A large number of theoretical [1–12] and experimental [13–24] works on double-resonance studies have been reported. The pump field is normally chosen from the radio frequency (rf) to the ultraviolet (uv) region. The saturation of the pump transition produces the level population and coherency effects [25], which result in signal enhancement and splitting of the probe transition known as Rabi splitting. The splitting is symmetric both in intensity and position with respect to the pump frequency. If the pump frequency is relatively low, the Doppler effect due to molecular (atomic) motion has a small effect on the line shape. However, if the pump frequency is relatively higher (e.g., ir, uv), the Doppler effect has a preponderant role on the signal line shape. The Doppler broadening effect may be removed using various techniques [26–32].

The theoretical studies on line shape are normally based on the solutions of optical Bloch equations [10,33–38], which may be derived from Liouville's equations of motion. The atom-field interactions are treated semiclassically to obtain the desired optical Bloch equations. The Hamiltonian of the system contains the unperturbed atomic and field Hamiltonian. The interaction part of the Hamiltonian arises from the interaction between a set of quantized nondegenerate atomic levels with the classical electromagnetic radiation. It is assumed that both the field frequencies are very nearly in resonance with the atomic transition frequencies. If two levels are closely spaced, a single pump radiation frequency may be used to saturate two nearby transitions, in which case one of the transitions may be on resonance. Thus a system with two closely spaced levels interacting with a single field is interesting from the high-resolution spectroscopic point of view. In fact,the presence of closely spaced levels affects the line shape considerably [36–38]. Closely spaced transitions are responsible for nonlinear-optical phenomena. Spectroscopy involving the closely spaced upper or lower levels has been reported in a number of theoretical papers [2,12,36–42]. The three-level system with two closely spaced upper levels was first studied by Schlossberg and Javan [2]. The saturation behavior of Doppler-broadened transitions was obtained by them. The effect of nonresonant interaction of a three-level atomic system with two closely spaced upper levels interacting with a single-mode running wave on the Doppler-free line shape was reported by us [36]. It was shown from numerical computations that the resonance peak frequencies are shifted. A very similar system under the influence of a standing-wave field has recently been reported [37]. The analytical expressions for shifts of the Lamb-dip peak frequencies and of the crossover resonance dip were obtained.

The interaction of a four-level atomic (molecular) system with two radiation fields has been studied numerically to obtain the line shape [38]. The effect of two intermediate closely spaced levels upon the two-photon resonances and on the Rabi splitting were studied. The two-photon transition caused by simultaneous absorption of

two photons is a nonlinear-optical phenomenon. The probability of two-photon absorption is proportional to the square of the field intensity. Hence the occurrence of two-photon resonance requires a high-power laser source. In this process the sum of the energies of two photons is equal to the energy difference between the two involved levels. These levels have the same parity. In other words, even a dipole-forbidden transition may be obtained via a two-photon resonance. The theory of two-photon resonances was first given by Göppert-Mayer [43]. Since then, a large number of theoretical as well as experimental studies have been published [44–50].

In a double-resonance process both one-photon and two-photon processes contribute to the signal line shape [1]. As the pump and signal frequencies need not be in resonance for two-photon absorption, the presence of a nearby level may affect the two-photon line shape. This is particularly true if there are two close-lying intermediate levels in the cascade-type double resonance and if the pump transition to and the signal transition from both of these levels are allowed. It may be noted that in molecular systems close-lying levels very commonly occur. Such systems may be quite complex. In our recent paper [38] we considered a relatively simpler case of close intermediate levels and presented a preliminary numerical solution. However, detailed analytical solution is necessary for interpretations of the two-photon resonances, frequency shift and Rabi splitting.

The steady-state optical Bloch equations for a four-level cascade-type system with two closely spaced intermediate levels interacting with two radiation fields are solved analytically to obtain the Doppler free signal line shape. In this calculation we assume that the amplitude of the signal field is much smaller compared to that of the pump radiation field. We present the results for different cases of on- and off-resonance pumping. The Rabi splitting for the on-resonance pumping is obtained. The two-photon resonances for off-resonance pumping are also presented. The effect of nearby levels on the two-photon resonance is discussed.

II. STEADY-STATE OPTICAL BLOCH EQUATIONS OF A FOUR-LEVEL ATOMIC SYSTEM

We consider an ensemble of nondegenerate four-level atomic or molecular systems (Fig. 1). The system interacts with two coherent monochromatic radiation fields. The pump frequency Ω_p is very nearly equal to the transition frequencies $\omega_1=(E_b-E_a)/\hbar$ and $\omega_2=(E_c-E_a)/\hbar$. This condition may only be achieved if ω_1 and ω_2 are very close to each other; for which the energy gap $\omega_2-\omega_1=\Delta$ is small. The signal frequency induces transitions across the energy-level difference associated with the transition frequencies $\omega_3=(E_d-E_b)/\hbar$ and $\omega_4=(E_d-E_c)/\hbar$. The detunings

$$\Delta\omega_1=\Omega_p-\omega_1 , \tag{1a}$$

$$\Delta\omega_2=\Omega_p-\omega_2 , \tag{1b}$$

$$\Delta\omega_3=\Omega_s-\omega_3 , \tag{1c}$$

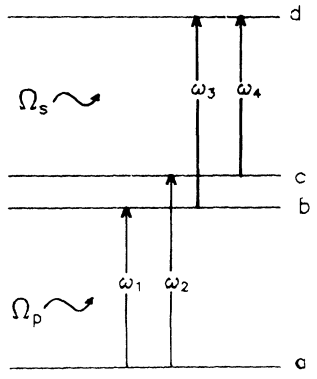

FIG. 1. Energy-level diagram of a four-level atom interacting with two fields.

and

$$\Delta\omega_4=\Omega_s-\omega_4 \tag{1d}$$

are very small. Thus we have a four-level double-resonance system with two closely spaced intermediate levels. We define the Rabi frequencies as

$$x_1=\epsilon_p\mu_{ab}/\hbar , \tag{2a}$$

$$x_2=\epsilon_p\mu_{ac}/\hbar , \tag{2b}$$

$$x_3=\epsilon_s\mu_{bd}/\hbar , \tag{2c}$$

and

$$x_4=\epsilon_s\mu_{cd}/\hbar , \tag{2d}$$

where ϵ_p and ϵ_s are the electric-field amplitudes of pump and signal radiations, respectively. The parameter μ_{ab} is the transition moment between the levels a and b. Similarly μ_{ac}, μ_{bd} and μ_{cd} are other transition moments. The transitions between the levels a and d and between the levels b and c are dipole forbidden. Hence there is no Rabi frequency associated with them. Thus the Hamiltonian of the system can be expressed as

$$H=H_0-2\mu\epsilon_p\cos(\Omega_p t)-2\mu\epsilon_s\cos(\Omega_s t) . \tag{3}$$

The Liouville equations of motion for the density matrix elements are given by

$$i\hbar\frac{\partial}{\partial t}\rho_{aa}=-\epsilon_p(\mu_{ab}\rho_{ba}+\mu_{ac}\rho_{ca}-\rho_{ab}\mu_{ba}-\rho_{ac}\mu_{ca}) , \tag{4}$$

$$i\hbar\frac{\partial}{\partial t}\rho_{bb}=-\epsilon_p(\mu_{ba}\rho_{ab}-\rho_{ba}\mu_{ab})-\epsilon_s(\mu_{bd}\rho_{db}-\rho_{bd}\mu_{db}) , \tag{5}$$

$$i\hbar\frac{\partial}{\partial t}\rho_{cc}=-\epsilon_p(\mu_{ca}\rho_{ac}-\rho_{ca}\mu_{ac})-\epsilon_s(\mu_{cd}\rho_{dc}-\rho_{cd}\mu_{dc}) , \tag{6}$$

$$i\hbar\frac{\partial}{\partial t}\rho_{dd}=-\epsilon_s(\mu_{db}\rho_{bd}+\mu_{dc}\rho_{cd}-\rho_{db}\mu_{bd}-\rho_{dc}\mu_{cd}) , \tag{7}$$

$$i\hbar\frac{\partial}{\partial t}\rho_{ab}=-\hbar\Delta\omega_1\rho_{ab}-\epsilon_p(\mu_{ab}\rho_{bb}+\mu_{ac}\rho_{cb}-\rho_{ad}\mu_{ab})+\epsilon_s\rho_{ad}\mu_{db} , \tag{8}$$

$$i\hbar\frac{\partial}{\partial t}\rho_{ac}=\hbar\Delta\omega_2\rho_{ac}-\epsilon_p(\mu_{ab}\rho_{bc}+\mu_{ac}\rho_{cc}-\rho_{aa}\mu_{ac})+\epsilon_s\rho_{ad}\mu_{dc}\ , \tag{9}$$

$$i\hbar\frac{\partial}{\partial t}\rho_{ad}=\hbar(\Delta\omega_1+\Delta\omega_3)\rho_{ad}-\epsilon_p(\mu_{ab}\rho_{bd}+\mu_{ac}\rho_{cd})+\epsilon_s(\rho_{ab}\mu_{bd}+\rho_{ac}\mu_{cd})\ , \tag{10}$$

$$i\hbar\frac{\partial}{\partial t}\rho_{bc}=\hbar(\Delta\omega_2-\Delta\omega_1)\rho_{bc}-\epsilon_p(\mu_{ba}\rho_{ac}-\rho_{ba}\mu_{ac})-\epsilon_s(\mu_{bd}\rho_{dc}-\rho_{bd}\mu_{dc})\ , \tag{11}$$

$$i\hbar\frac{\partial}{\partial t}\rho_{bd}=\hbar\Delta\omega_3\rho_{bd}-\epsilon_p\mu_{ba}\rho_{ad}-\epsilon_s(\mu_{bd}\rho_{dd}-\rho_{bb}\mu_{bd}-\rho_{bc}\mu_{cd})\ , \tag{12}$$

$$i\hbar\frac{\partial}{\partial t}\rho_{cd}=\hbar\Delta\omega_4\rho_{cd}-\epsilon_s(\mu_{cd}\rho_{dd}-\rho_{cb}\mu_{bd}-\rho_{cc}\mu_{cd})-\epsilon_p\rho_{ca}\mu_{ad}\ . \tag{13}$$

In the derivation of the Liouville equations we have assumed $\Omega_s-\Omega_p$ is fairly large, which ensures the use of the rotating-wave approximation (RWA). The polarizations associated with the pump transitions are given by

$$P_{1r}+iP_{1i}=N\mu_{ba}\rho_{ab}\ , \tag{14a}$$

$$P_{2r}+iP_{2i}=N\mu_{ca}\rho_{ac}\ , \tag{14b}$$

$$P_{3r}+iP_{3i}=N\mu_{bd}\rho_{db}\ , \tag{14c}$$

and

$$P_{4r}+iP_{4i}=N\mu_{cd}\rho_{dc}\ , \tag{14d}$$

where N is the number of atoms per unit volume. The population differences are

$$\Delta N_1=N(\rho_{aa}-\rho_{bb})\ , \tag{15a}$$

$$\Delta N_2=N(\rho_{aa}-\rho_{cc})\ , \tag{15b}$$

$$\Delta N_3=N(\rho_{bb}-\rho_{dd})\ , \tag{15c}$$

and

$$\Delta N_4=N(\rho_{cc}-\rho_{dd})\ . \tag{15d}$$

The polarizations defined in Eq. (14) are associated with the allowed transitions. The transitions between levels b and c and those between levels a and d are dipole forbidden, since $\mu_{bc}=\mu_{ad}=0$. However, ρ_{bc} and ρ_{ad} are not zero. The time rate of change of these matrix elements [Eqs. (10) and (11)] are obtained from the rate of change of other density matrix elements. This will involve terms like

$$P_{nr}+iP_{ni}=N\mu_{ca}\mu_{ab}\rho_{bc} \tag{16a}$$

and

$$P_{mr}+iP_{mi}=N\mu_{db}\mu_{ba}\rho_{ad}\ . \tag{16b}$$

The significance of the terms P_{nr}, P_{ni}, P_{mr} and P_{mi} is shown in Fig. 2. It is clear that the dipole transitions between the levels a and b and between the levels a and c

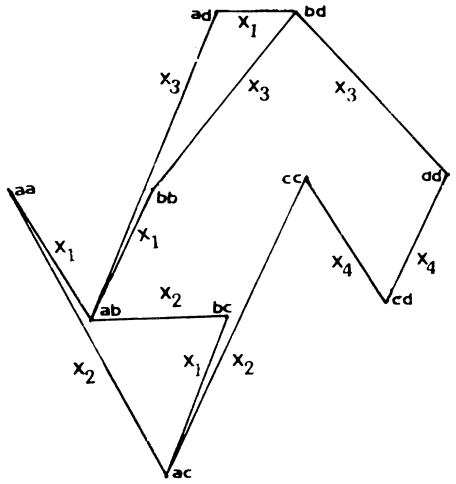

FIG. 2. Diagrammatic representation of transitions. The transitions $a\rightarrow b$, $a\rightarrow c$, $b\rightarrow d$, and $c\rightarrow d$ depend on x_1^2, x_2^2, x_3^2, and x_4^2, respectively, whereas the paths b to c and a to d depend on $x_1^2x_2^2$ and $x_1^2x_3^2$, respectively. aa, ab, etc. signify the elements of the density matrix ρ.

may be obtained through x_1^2 and x_2^2, respectively. Similarly, the transitions $b\rightarrow d$ and $c\rightarrow d$ involve x_3 and x_4, respectively. The transitions $b\rightarrow c$ and $a\rightarrow d$ are dipole forbidden. However, it is clear from Fig. 2 that the passage from ρ_{bb} to ρ_{cc} may be achieved through the path involving $x_1^2x_2^2$. Similarly, the path $a\rightarrow d$ involves $x_1^2x_3^2$. It may be checked that other paths for these passages may be obtained through the terms $x_1x_2x_3x_4$. By using the Eqs. (4)–(16) we obtain 15 optical Bloch equations in terms of polarizations, nonlinear terms P_n, P_m and the population differences. The steady-state optical Bloch equations after adding phenomenological relaxation constants are

$$\Delta\omega_1P_{1i}+\frac{\epsilon_p}{\hbar}P_{ni}+\frac{\epsilon_s}{\hbar}P_{mi}-\frac{P_{1r}}{T_2}=0\ , \tag{17}$$

$$-\Delta\omega_1P_{1r}-\frac{\epsilon_p}{\hbar}|\mu_{ab}|^2\Delta N_1+\frac{\epsilon_p}{\hbar}P_{nr}-\frac{\epsilon_s}{\hbar}P_{mr}-\frac{P_{1i}}{T_2}=0\ , \tag{18}$$

$$\Delta\omega_2P_{2i}-\frac{\epsilon_p}{\hbar}P_{ni}+\frac{\epsilon_s}{\hbar}\frac{\mu_{dc}\mu_{ca}}{\mu_{db}\mu_{ba}}P_{mi}-\frac{P_{2r}}{T_2}=0\ , \tag{19}$$

$$-\Delta\omega_2P_{2r}-\frac{\epsilon_p}{\hbar}|\mu_{ac}|^2\Delta N_2+\frac{\epsilon_p}{\hbar}P_{nr}-\frac{\epsilon_s}{\hbar}\frac{\mu_{dc}\mu_{ca}}{\mu_{db}\mu_{ba}}P_{mr}-\frac{P_{2i}}{T_2}=0\ , \tag{20}$$

$$\Delta\omega_3P_{3i}-\frac{\epsilon_p}{\hbar}P_{mi}+\frac{\epsilon_s}{\hbar}\frac{\mu_{cd}\mu_{db}}{\mu_{ca}\mu_{ab}}P_{ni}-\frac{P_{3r}}{T_2}=0\ , \tag{21}$$

$$-\Delta\omega_3P_{3r}-\frac{\epsilon_p}{\hbar}|\mu_{bd}|^2\Delta N_3+\frac{\epsilon_p}{h}P_{mr}-\frac{\epsilon_s}{\hbar}\frac{\mu_{cd}\mu_{db}}{\mu_{ca}\mu_{ab}}P_{nr}-\frac{P_{3i}}{T_2}=0\ , \tag{22}$$

$$\Delta\omega_4 P_{4i}-\frac{\epsilon_s}{\hbar}\frac{\mu_{bd}\mu_{dc}}{\mu_{ca}\mu_{ab}}P_{ni}-\frac{\epsilon_p}{\hbar}\frac{\mu_{dc}\mu_{ca}}{\mu_{db}\mu_{ba}}P_{mi}-\frac{P_{4r}}{T_2}\ , \tag{23}$$

$$\Delta\omega_4 P_{4r}-\frac{\epsilon_p}{\hbar}\frac{\mu_{dc}\mu_{ca}}{\mu_{db}\mu_{ba}}P_{mr}+\frac{\epsilon_s}{\hbar}|\mu_{cd}|^2(\Delta N_1+\Delta N_3-\Delta N_2)+\frac{\epsilon_s}{\hbar}\frac{\mu_{bd}\mu_{dc}}{\mu_{ca}\mu_{ab}}P_{nr}+\frac{P_{4i}}{T_2}=0\ , \tag{24}$$

$$\frac{4\epsilon_p}{\hbar}P_{1i}+\frac{2\epsilon_p}{\hbar}P_{2i}-\frac{2\epsilon_s}{\hbar}P_{3i}-\frac{(\Delta N_1-\Delta N_{10})}{T_1}=0\ , \tag{25}$$

$$\frac{4\epsilon_p}{\hbar}P_{2i}+\frac{2\epsilon_p}{\hbar}P_{1i}-\frac{2\epsilon_s}{\hbar}P_{4i}-\frac{(\Delta N_2-\Delta N_{20})}{T_1}=0\ , \tag{26}$$

$$\frac{4\epsilon_s}{\hbar}P_{3i}+\frac{2\epsilon_s}{\hbar}P_{4i}-\frac{2\epsilon_p}{\hbar}P_{1i}-\frac{(\Delta N_3-\Delta N_{30})}{T_1}=0\ , \tag{27}$$

$$(\Delta\omega_2-\Delta\omega_1)P_{ni}-\frac{\epsilon_p}{\hbar}|\mu_{ab}|^2P_{2i}-\frac{\epsilon_p}{\hbar}|\mu_{ac}|^2P_{1i}+\frac{\epsilon_s}{\hbar}\frac{\mu_{ca}\mu_{ab}\mu_{bd}}{\mu_{cd}}P_{4i}+\frac{\epsilon_s}{\hbar}\frac{\mu_{dc}\mu_{ca}\mu_{ab}}{\mu_{db}}P_{3i}-\frac{P_{nr}}{T_2}=0\ , \tag{28}$$

$$-(\Delta\omega_2-\Delta\omega_1)P_{nr}+\frac{\epsilon_p}{\hbar}|\mu_{ab}|^2P_{2r}-\frac{\epsilon_p}{\hbar}|\mu_{ac}|^2P_{1r}+\frac{\epsilon_s}{\hbar}\frac{\mu_{ca}\mu_{ab}\mu_{bd}}{\mu_{cd}}P_{4r}-\frac{\epsilon_s}{\hbar}\frac{\mu_{dc}\mu_{ca}\mu_{ab}}{\mu_{db}}P_{3r}-\frac{P_{ni}}{T_2}=0\ , \tag{29}$$

$$(\Delta\omega_1+\Delta\omega_3)P_{mi}-\frac{\epsilon_p}{\hbar}|\mu_{ab}|^2P_{3i}+\frac{\epsilon_s}{\hbar}|\mu_{bd}|^2P_{1i}-\frac{\epsilon_p}{\hbar}\frac{\mu_{db}\mu_{ba}\mu_{ac}}{\mu_{dc}}P_{4i}+\frac{\epsilon_s}{\hbar}\frac{\mu_{cd}\mu_{db}\mu_{ba}}{\mu_{ca}}P_{2i}-\frac{P_{mr}}{T_2}=0\ , \tag{30}$$

$$-(\Delta\omega_1+\Delta\omega_3)P_{mr}+\frac{\epsilon_p}{\hbar}|\mu_{ab}|^2P_{3r}-\frac{\epsilon_s}{\hbar}|\mu_{bd}|^2P_{1r}+\frac{\epsilon_p}{\hbar}\frac{\mu_{db}\mu_{ba}\mu_{ac}}{\mu_{dc}}P_{4r}-\frac{\epsilon_s}{\hbar}\frac{\mu_{cd}\mu_{db}\mu_{ba}}{\mu_{ca}}P_{2r}-\frac{P_{mi}}{T_2}=0\ . \tag{31}$$

The parameters T_1 and T_2 are the longitudinal and transverse relaxational constants. The population differences ΔN_i associated with the diagonal matrix elements ρ_{ii} relax to their equilibrium values ΔN_{i0} with time T_1. Since the energy gap Δ is very small compared to the transition frequencies ω_1 and ω_2, the values of ΔN_{10} and ΔN_{20} are assumed to be equal. However, the value of ΔN_{30} is very small compared to ΔN_{10} and ΔN_{20}. The remaining off-diagonal matrix elements relax to their equilibrium zero values with time period T_2.

III. SIGNAL LINE SHAPE

We present the analytical solution for the total signal polarization

$$P_i=P_{3i}+P_{4i}\ . \tag{32}$$

The analytical closed-form expressions for P_{3i} and P_{4i} are very complicated and are given in the Appendix. To get simpler closed-form expression for P_{3i} and P_{4i} we shall assume the Rabi frequencies $x_1=x_2=x$ and $x_3=x_4=x_s$. The relaxation parameters $T_1=T_2=T$. In the present work the pump electric-field amplitude is much higher than the signal electric-field amplitude; i.e., $\epsilon_p \gg \epsilon_s$. This leads to $x \gg x_s$. Hence the signal polarization is

$$P_i=C\left[-\frac{1}{1+\Delta\omega_3^2T^2+x^2T^2\left[1-\frac{T^2(\Delta\omega_1+2\Delta\omega_3)^2}{1+(\Delta\omega_1+\Delta\omega_3)^2T^2+2x^2T^2}\right]}-\frac{1}{1+\Delta\omega_4^2T^2+x^2T^2\left[1-\frac{T^2(\Delta\omega_2+2\Delta\omega_4)^2}{1+(\Delta\omega_2+\Delta\omega_4)^2T^2+2x^2T^2}\right]}\right.$$
$$+x^2T^2\frac{1}{1+\Delta\omega_3^2T^2+x^2T^2\left[1-\frac{T^2(\Delta\omega_1+2\Delta\omega_3)^2}{1+(\Delta\omega_1+\Delta\omega_3)^2T^2+2x^2T^2}\right]}$$
$$\times\frac{1}{1+\Delta\omega_4^2T^2+x^2T^2\left[1-\frac{T^2(\Delta\omega_2+2\Delta\omega_4)^2}{1+(\Delta\omega_2+\Delta\omega_4)^2T^2+2x^2T^2}\right]}$$
$$\left.\times\left[2-\frac{T^2(\Delta\omega_1+2\Delta\omega_3)(\Delta\omega_2+2\Delta\omega_4)}{1+(\Delta\omega_1+\Delta\omega_3)^2T^2+2x^2T^2}-\frac{T^2(\Delta\omega_1+2\Delta\omega_3)(\Delta\omega_2+2\Delta\omega_4)}{1+(\Delta\omega_2+\Delta\omega_4)^2T^2+2x^2T^2}\right]\right]$$
$$=P_i^{(1)}+P_i^{(2)}+P_i^{(3)}\ , \tag{33}$$

where the expressions for P_{3i} and P_{4i} are used from the Appendix. The parameter C is proportional to ΔN_{30} and μ_{bd}. In the derivation of Eq. (33) we have retained the first significant nonlinear contribution arising from the square of the pump Rabi frequency x. Similar nonlinear terms arising from the signal Rabi frequency have been neglected, since they are very small compared to their pump Rabi frequency counterpart. The first term in Eq. (33) contains the Lorentzian line shape arising from the transition $b \rightarrow d$. The second term includes the Lorentzi-

an arising from the transition $c \rightarrow d$. In addition to the one-photon transitions giving the Lorentzians, these two terms also contain a contribution to two-photon absorption. The third term has a higher-order contribution with respect to the electric field ϵ_p. The following cases of on- and off-resonance pumping are relevant.

A. Case I: $\Omega_p = \omega_1$

When the pump frequency is in resonance with the transition frequency ω_1, the detuning $\Delta\omega_1 = 0$ and $\Delta\omega_2 = -\Delta$. The first term in Eq. (33) reduces to

$$P_i^{(1)}(\Delta\omega_3) = -\frac{C}{1+\Delta\omega_3^2 T^2 + x^2 T^2 \left[1 - \frac{4\Delta\omega_3^2 T^2}{1+\Delta\omega_3^2 T^2 + 2x^2 T^2}\right]} . \tag{34}$$

To find the extremum of the function $P_i^{(1)}(\Delta\omega_3)$, the first derivative of $P_i^{(1)}(\Delta\omega_3)$ with respect to $\Delta\omega_3$ is made equal to zero. Thus we are left with the following equation:

$$\Delta\omega_3 \left[\Delta\omega_3^4 + \frac{(4+8x^2T^2)}{T^2}\Delta\omega_3^2 + \frac{2-8x^4T^4}{T^4}\right] = 0 . \tag{35}$$

We find that the equation in parentheses has one real positive root and one real negative root. The remaining two roots are complex, and we are not concerned with them. Hence Eq. (35) has three extrema for

$$\Delta\omega_3 = 0 \tag{36a}$$

and

$$\Delta\omega_{3\pm} = \pm \left[\frac{-(2+4x^2T^2) + \sqrt{2+16x^2T^2+24x^4T^4}}{T^2}\right]^{1/2} . \tag{36b}$$

It is easy to check that $\Delta\omega_3 = 0$ gives a maximum and the other two roots lead to two minima [Eq. (36b)]. Thus Eq. (33) shows two peaks separated by $\Delta\omega_{3+}$ with respect to the intermediate maximum at $\Delta\omega_3 = 0$. These two peaks are at equal distance with respect to the central ($\Delta\omega_3 = 0$) position. The separation between the two peaks increases with the increase of xT. These two peaks are commonly known as Rabi components and occur if the pump is in the on-resonance condition. The magnitude of Rabi splitting depends on the value of xT. The above equation (36b) shows that Rabi splitting vanishes when $xT = 1/\sqrt{2}$. For lower values of xT, this splitting is not observed.

The condition $\Delta\omega_1 = 0$ reduces the second term to

$$P_i^{(2)} = -\frac{C}{1+(\Delta\omega_3+\Delta)^2 T^2 + x^2 T^2 \left[1 - \frac{T^2(\Delta+2\Delta\omega_3)^2}{1+\Delta\omega_3^2 T^2 + 2x^2 T^2}\right]} , \tag{37}$$

where $\Delta\omega_4 = \Delta + \Delta\omega_3$ and $\Delta\omega_2 = -\Delta$ have been substituted. ΔT is moderately high compared to unity (in our computation we shall use $\Delta T \sim 15$). Hence $P_i^{(2)}$ contributes nothing unless $\Delta\omega_3 \sim -\Delta$, which is the on-resonance condition for the second Lorentzian peak. Thus $P_i^{(2)}$ has a small contribution when the signal is nearly resonant with ω_3. The effect of the third term is also very small.

B. Case II: $\Omega_p = \omega_2$

This is the particular case for which $\Delta\omega_2 = 0$ may be treated exactly as in the case for $\Delta\omega_1 = 0$. The only difference is that the result deduced for $\Delta\omega_3 = 0$ in the earlier section should be replaced by those for $\Delta\omega_4 = 0$.

C. Case III: $\omega_1 < \Omega_p < \omega_2$

When the pump frequency is intermediate between the resonance frequencies ω_1 and ω_2, one can observe two-photon resonances satisfying the condition $\Delta\omega_1 + \Delta\omega_3 = 0$ or $\Delta\omega_2 + \Delta\omega_4 = 0$. When $\Delta\omega_1 + \Delta\omega_3 = 0$,

$$P_i = C\left[-\frac{1}{1+\Delta\omega_1^2 T^2 + x^2 T^2\left[1 - \frac{\Delta\omega_1^2 T^2}{1+2x^2T^2}\right]} - \frac{1}{1+\Delta\omega_2^2 T^2 + x^2 T^2\left[1 - \frac{\Delta\omega_2^2 T^2}{1+2x^2T^2}\right]}\right.$$
$$\left. + 2x^2T^2 \frac{1}{1+\Delta\omega_1^2 T^2 + x^2 T^2\left[1 - \frac{\Delta\omega_1^2 T^2}{1+2x^2T^2}\right]} \frac{1}{1+\Delta\omega_2^2 T^2 + x^2 T^2\left[1 - \frac{\Delta\omega_2^2 T^2}{1+2x^2T^2}\right]}\left[1 - \frac{\Delta\omega_1\Delta\omega_2 T^2}{1+2x^2T^2}\right]\right] . \tag{38}$$

When $\Omega_p = (\omega_1+\omega_2)/2$, $\Delta\omega_1 = \Delta/2$, and $\Delta\omega_2 = -\Delta/2$,

$$P_i = C\left[-\frac{2}{1+\frac{\Delta^2T^2}{4}+x^2T^2\left[1-\frac{\Delta^2T^2/4}{1+2x^2T^2}\right]} + \frac{2x^2T^2}{\left[1+\frac{\Delta^2T^2}{4}+x^2T^2\left[1-\frac{\Delta^2T^2/4}{1+2x^2T^2}\right]\right]^2} \times \left[1+\frac{\Delta^2T^2/4}{1+2x^2T^2}\right]\right] . \quad (39)$$

It is easy to check from Eq. (38) that the contributions to the two-photon intensities from the first and second terms are higher compared to the contribution of the third term. The effect of the third term is opposite those of the first two terms and tends to reduce the intensity of two-photon resonances. This is because $\Delta\omega_1$ and $\Delta\omega_2$ are opposite in sign when the pump frequency is in the region $\omega_1 < \Omega_p < \omega_2$. When the pump frequency is $\Omega_p = (\omega_1+\omega_2)/2$ [Eq. (39)], this reduction of the two-photon effect is maximum.

D. Case IV: $\Omega_p < \omega_1$ and $\Omega_p > \omega_2$

The fourth case for which the pump frequency is $\Omega_p < \omega_1$ or $\Omega_p > \omega_2$ is different from the third case. In the present case $\Delta\omega_1$ and $\Delta\omega_2$ bear the same sign. Therefore, the contribution of the third term in Eq. (38) is to enhance the two-photon effect. Thus the two-photon resonances for these cases persist even for a fairly large (0.1 MHz) detuning.

IV. CALCULATION OF SIGNAL LINE SHAPE

In our computation we consider that the spacing between the closely spaced levels is 0.15 MHz. The pump and signal frequencies are of the order of 10000 and 15000 MHz, respectively. Thus our system is an ideal four-level cascade-type microwave-microwave (MW-MW) double-resonance system. The Rabi frequencies and the relaxation constants are chosen in such a way that they are close to an experimental situation. The signal line shapes for $x = 0.01$ MHz and $T = 100$ μs are exhibited for various pump frequencies. When the pump is in resonance with one of the transitions $a \rightarrow b$ or $a \rightarrow c$, we obtain the Rabi splitting (Fig. 3). The split Rabi components are asymmetric in intensities. The asymmetry of the Rabi components decreases when the energy gap between the closely spaced intermediate levels is sufficiently increased (Fig. 4). In these cases the values of $x = 0.01$ MHz and $T = 100$ μs remain unchanged. The asymmetry also vanishes when one of the transition moments μ_{bd} or μ_{cd} is weaker relative to the other [38]. Hence, the asymmetry of the Rabi components originates from the nearby transition. As the pump frequency is intermediate between the transition frequencies ω_1 and ω_2, a small two-photon absorption is obtained (Fig. 5). It is very interesting to observe that the intensity of the two-photon signal becomes weak and tend to vanish at $\Omega_p = (\omega_1+\omega_2)/2$ (Fig. 6). This may be understood on the basis of our previous discussions. An important feature of two-photon absorption is the faster vanishing intensity when the pump frequency is in the range $\omega_1 < \Omega_p < \omega_2$ (Figs. 5 and 6). As explained earlier, this may happen due to the effect of nearby one-photon transitions. In this case the contribution of the third term in Eq. (38) expressed in terms of the product of the Lorentzians of the two resonances is to diminish the intensity of two-photon resonance. Eventually at $\Omega_p = (\omega_1+\omega_2)/2$ this term contributes significantly [Eq. (39)] and tends to cancel the two-photon resonances almost entirely [Fig. 6(b)]. Hence the nearby transition affects the two-photon resonances considerably. The occurrence of the two-photon absorption peak is also reported when $\Omega_p > \omega_2$ [Fig. 7(a)], as well as $\Omega_p < \omega_1$ [Fig. 7(b)]. The intensity of two-photon resonance increases with the increase of the pump Rabi frequency x (Fig. 8).

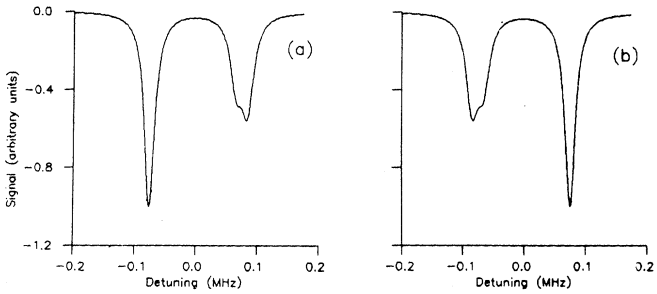

FIG. 3. Signal polarization P_i vs detuning $\Omega_s - (\omega_3+\omega_4)/2$, $\Delta = 0.15$, $T^{-1} = 0.01$, $x = 0.01$ MHz; $\omega_1 = 9999.925$ and $\omega_3 = 15000.0$ MHz. (a) $\Delta\omega_1 = 0.0$ and (b) $\Delta\omega_1 = 0.15$ MHz.

Figure 9 exhibits the shifts of the Lorentzian peaks corresponding to the two transitions for a pump frequency $\Omega_p = (\omega_1+\omega_2)/2$. In these calculations we have assumed $T = 20.0$ μs and pump Rabi frequency between 0.01 and 0.03 MHz. The shift of the Lorentzian peak is such that they repel each other more and more as the Rabi frequency is increased. This intensity-dependent shift is very important in high-resolution laser spectroscopy.

The saturation effects of line shape have been presented in Fig. 10. It is clear that as the value of T is decreased

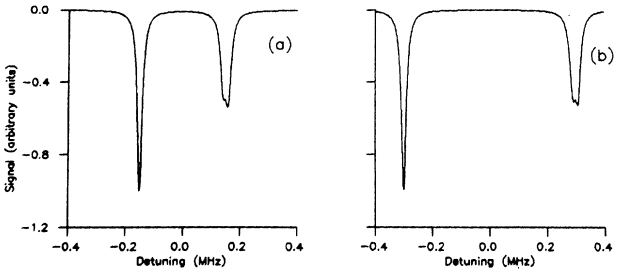

FIG. 4. Signal polarization P_i vs detuning $\Omega_s - (\omega_3+\omega_4)/2$, $T^{-1} = 0.01$, $x = 0.01$, $\Delta\omega_1 = 0.0$, and $\omega_3 = 15\,000.0$ MHz. (a) $\Delta = 0.3$, $\omega_1 = 9999.85$ MHz and (b) $\Delta = 0.6$, $\omega_1 = 9999.7$ MHz.

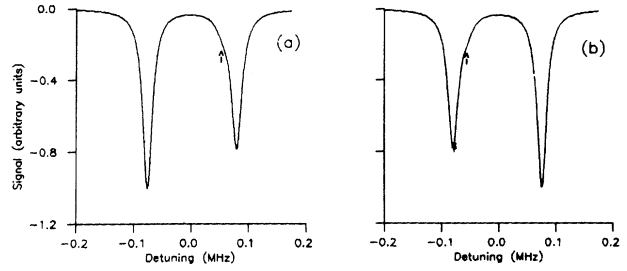

FIG. 5. Signal polarization P_i vs detuning $\Omega_s-(\omega_3+\omega_4)/2$, $\Delta=0.15$, $T^{-1}=0.01$, $x=0.01$, $\omega_1=9999.925$ and $\omega_3=15000.0$ MHz. (a) $\Delta\omega_1=0.015$ and (b) 0.135 MHz. The arrow indicates the presence of weak two-photon resonances.

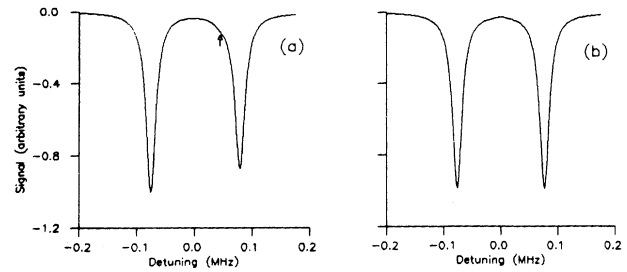

FIG. 6. Signal polarization P_i vs detuning $\Omega_s-(\omega_3+\omega_4)/2$, $\Delta=0.15$, $T^{-1}=0.01$, $x=0.01$, $\omega_1=9999.925$ and $\omega_3=15000.0$ MHz. (a) $\Delta\omega_1=0.025$ and (b) 0.075 MHz. The arrow indicates the presence of weak two-photon resonances.

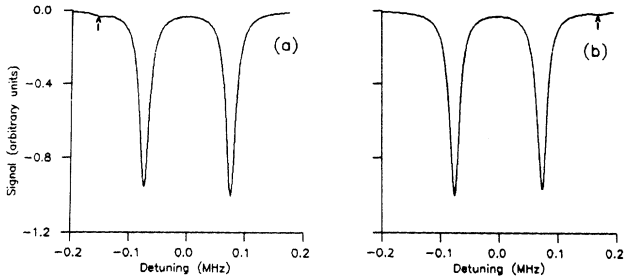

FIG. 7. Signal polarization P_i vs detuning $\Omega_s-(\omega_3+\omega_4)/2$, $\Delta=0.15$, $T^{-1}=0.01$, $x=0.01$, $\omega_1=9999.925$ and $\omega_3=15000.0$ MHz. (a) $\Delta\omega_1=0.35$ and (b) -0.1 MHz. The arrow indicates the presence of two-photon resonances.

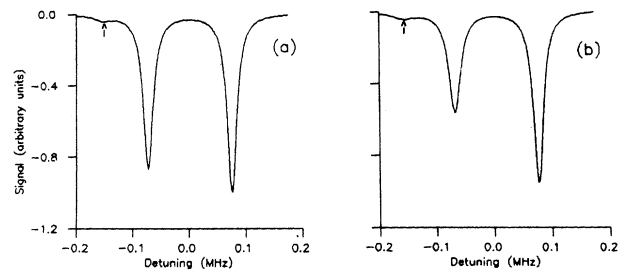

FIG. 8. Signal polarization P_i vs detuning $\Omega_s-(\omega_3+\omega_4)/2$, $\Delta=0.15$, $T^{-1}=0.01$, $\omega_1=9999.925$, $\omega_3=15000.0$ and $\Delta\omega_1=0.35$ MHz. (a) $x=0.015$ and (b) $x=0.025$ MHz. The arrow indicates the presence of weak two-photon resonances.

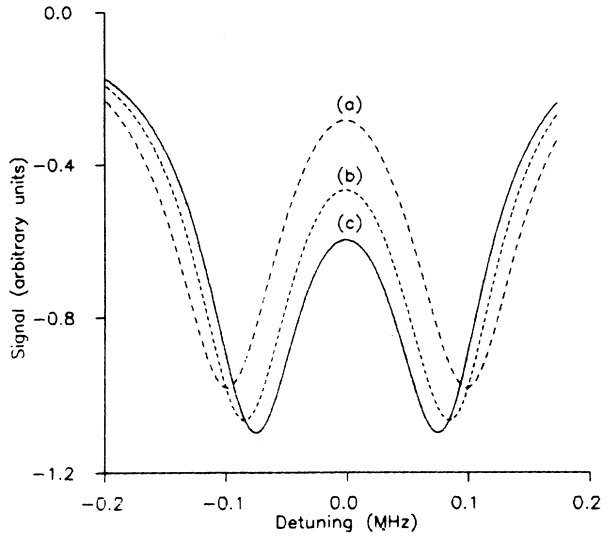

FIG. 9. Signal polarization P_i vs detuning $\Omega_s-(\omega_3+\omega_4)/2$, $\Delta=0.15$, $T^{-1}=0.5$, $\omega_1=9999.925$, $\omega_3=15000.0$ and $\Delta\omega_1=0.075$ MHz. (a) $x=0.05$, (b) $x=0.03$, and (c) $x=0.01$ MHz.

the two Lorentzians coalesce to form a single peak. Hence the peaks are no longer resolved in Fig. 10(c). In this calculation we have assumed that the pump frequency $\Omega_p=(\omega_1+\omega_2)/2$.

The calculation of signal line shape may be extended for P_n's and P_m's equal to zero. This assumption will lead to a great simplification of algebraic steps involving the expressions for P_{3i} and P_{4i}. In this case the asymmetry of the Rabi splitting, the frequency shift, and two-photon resonances are not observed. The results for P_n's equal to zero are not presented.

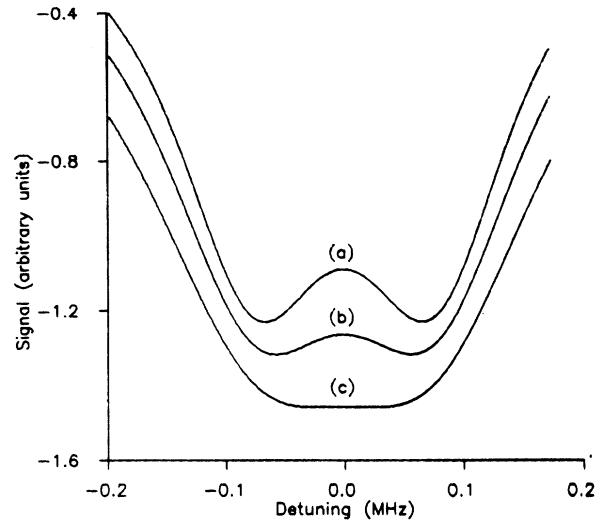

FIG. 10. Signal polarization P_i vs detuning $\Omega_s-(\omega_3+\omega_4)/2$, $\Delta=0.15$, $\omega_1=9999.925$, $\omega_3=15000.0$, $\Delta\omega_1=0.075$, $x=0.01$ MHz. (a) $T=12.0$, (b) $T=10.0$, and (c) $T=8.0\,\mu$s.

V. CONCLUSIONS

The analytical solutions of 15 Bloch equations are presented. In this calculation we have assumed that the pump electric field ϵ_p is much stronger than the signal electric field ϵ_s. This assumption is compatible with spectroscopic studies of double-resonance line shape. Hence the terms with higher power of ϵ_s or x_s have been neglected with respect to ϵ_p or x. In the expression of polarizations (33) only the odd power of electric field appears. This is because we are considering a gaseous medium which is inversion symmetric. The Doppler-broadening effects are not considered, since the calculations are restricted to the low-frequency region.

The line-shape calculation shows two-photon absorption in addition to the two one-photon Lorentzian peaks. The two-photon absorption is very sensitive to the pump frequencies. When the pump detunings $(\Omega_p-\omega_1)$ and $(\Omega_p-\omega_2)$ are made larger, the intensities of the two-photon resonances become smaller. The larger detuning from the single-photon transition means a shorter time of stay of the atom in the intermediate state after the absorption of the first photon. For a two-photon absorption to occur, the second photon should be absorbed during the time the atom stays in the intermediate state. Hence, the probability of two-photon transition is reduced [44]. It is very interesting that the two-photon absorption almost vanishes at $\Omega_p=(\omega_1+\omega_2)/2$. The vanishing of two-photon resonance at $\Omega_p=(\omega_1+\omega_2)/2$ is due to the cancellation effects arising from the contribution of the third term in Eq. (33). It is to be noted that for $\omega_1<\Omega_p<\omega_2$, the contribution of the third term is the opposite in nature with respect to $P_i^{(1)}$ and $P_i^{(2)}$. Thus the two-photon effects appear to be vanishing faster for pump frequency lying between $\omega_1<\Omega_p<\omega_2$. However, the term $P_i^{(3)}$ is unable to dominate over the contributions arising from $P_i^{(1)}$ and $P_i^{(2)}$. At $\Omega_p=(\omega_1+\omega_2)/2$, the contributions of $P_i^{(1)}$ and $P_i^{(2)}$ are minimum and thus the effects of two-photon resonance almost disappear. The near vanishing of the two-photon resonance in the region $\omega_1<\Omega_p<\omega_2$ may be due to the effect of the nearby transition. Actually, in our numerical computation [38] we showed that when the signal Rabi frequencies $x_3\gg x_4$ or $x_4\gg x_3$, the two-photon resonances were observed even for $\Omega_p=(\omega_1+\omega_2)/2$.

The Rabi splitting is obtained when $\Omega_p=\omega_1$ or $\Omega_p=\omega_2$. The intensities of the two Rabi components are unequal for both cases. In our earlier paper we reported symmetric Rabi splitting when one of the transition moments μ_{bd} or μ_{cd} is much smaller compared to μ_{cd} or μ_{bd}, respectively. In other words, when one of the transitions connected by the signal field is substantially weak, the Rabi components are symmetric. These results manifest the effect of the nearby transitions on the Rabi splittings.

The nonlinear effects, which include the Rabi splitting and the shifts of Lorentzian peak frequencies, appear through the terms P_n's and P_m's in our calculation. The data used for computation have been chosen in such a way that they are compatible with the real experimental situation. However, an accurate line-shape simulation is possible only if the information about x,x_s, T_1 and T_2 is known.

APPENDIX

The expression for P_{mi} may be found from Eqs. (1), (3), (5), (19), and (20). This is given by

$$P_{mi}=-\frac{\epsilon_s}{\hbar}T^2|\mu_{bd}|^2\left[(2\Delta\omega_1+\Delta\omega_3)\frac{P_{1i}}{D_1}-(\Delta\omega_1+\Delta\omega_2+\Delta\omega_3)\frac{P_{2i}}{D_1}\right]+\frac{\epsilon_p}{\hbar}T^2|\mu_{ab}|^2\left[(\Delta\omega_1+2\Delta\omega_3)\frac{P_{3i}}{D_1}-(\Delta\omega_1+\Delta\omega_3+\Delta\omega_4)\frac{P_{4i}}{D_1}\right]. \tag{A1}$$

In a similar way, P_{ni} is found to be

$$P_{ni}=-\frac{\epsilon_p}{\hbar}T^2|\mu_{ab}|^2\left[(\Delta+\Delta\omega_1)\frac{P_{1i}}{D}+(\Delta-\Delta\omega_2)\frac{P_{2i}}{D}-\frac{1}{k}(\Delta-\Delta\omega_3)\frac{P_{3i}}{D}+\frac{1}{k}(\Delta+\Delta\omega_4)\frac{P_{4i}}{D}\right], \tag{A2}$$

where $k=\epsilon_p/\epsilon_s$. The parameters D and D_1 are given by

$$D=1+\Delta^2T^2+2(x_1^2+x_3^2)T^2 \tag{A3}$$

and

$$D_1=1+(\Delta\omega_1+\Delta\omega_3)^2T^2+2(x_1^2+x_3^2)T^2\ . \tag{A4}$$

The polarization P_{1i} associated with levels 1 and 2 is given by

$$P_{1i}=-\frac{\epsilon_p}{\hbar}T^2|\mu_{ab}|^2\frac{\Delta N_{10}}{D_3}-\frac{M_1}{D_3}P_{2i}+\frac{M_2}{D_3}P_{3i}+\frac{M_3}{D_3}P_{4i}\ , \tag{A5}$$

where

$$M_1=x_1^2T^2\left[3-\frac{T^2}{D}(\Delta+\Delta\omega_1)(\Delta-\Delta\omega_2)\right]+x_3^2T^2\left[1-\frac{T^2}{D_1}(2\Delta\omega_1+\Delta\omega_3)(\Delta\omega_1+\Delta\omega_2+\Delta\omega_3)\right], \tag{A6}$$

$$M_2 = x_1^2 \frac{T^2}{k}\left[4-\frac{T^2}{D}(\Delta+\Delta\omega_1)(\Delta-\Delta\omega_3) - \frac{T^2}{D_1}(\Delta\omega_1+2\Delta\omega_3)(2\Delta\omega_1+\Delta\omega_3)\right], \quad \text{(A7)}$$

$$M_3 = x_1^2 \frac{T^2}{k}\left[2-\frac{T^2}{D}(\Delta+\Delta\omega_1)(\Delta+\Delta\omega_4) - \frac{T^2}{D_1}(2\Delta\omega_1+\Delta\omega_3)(\Delta\omega_1+\Delta\omega_3+\Delta\omega_4)\right], \quad \text{(A8)}$$

and

$$D_3 = 1+\Delta\omega_1^2T^2+x_1^2T^2\left[5-\frac{T^2}{D}(\Delta+\Delta\omega_1)^2\right] + x_3^2T^2\left[1-\frac{T^2}{D_1}(2\Delta\omega_1+\Delta\omega_3)^2\right]. \quad \text{(A9)}$$

The polarization P_{2i} arises due to the transition a-c. The expression for P_{2i} in terms of P_{3i} and P_{4i} is given by

$$P_{2i} = \frac{X_1}{D_4} + \frac{X_2}{D_4}P_{3i} + \frac{X_3}{D_4}P_{4i}, \quad \text{(A10)}$$

where

$$X_1 = -\frac{\epsilon_p}{\hbar}T|\mu_{ab}|^2\frac{\Delta N_{20}}{D_5} + \frac{\epsilon_p}{\hbar}T|\mu_{ab}|^2\frac{1}{D_3D_5}\left[x_1^2T^2\left[3-\frac{T^2}{D}(\Delta+\Delta\omega_1)(\Delta-\Delta\omega_2)\right] + x_3^2T^2\left[1-\frac{T^2}{D_1}(2\Delta\omega_1+\Delta\omega_3)(\Delta\omega_1+\Delta\omega_2+\Delta\omega_3)\right]\right], \quad \text{(A11)}$$

$$X_2 = \frac{1}{kD_5}x_1^2T^2\left[2-\frac{T^2}{D_1}(\Delta\omega_1+2\Delta\omega_3)(\Delta\omega_1+\Delta\omega_2+\Delta\omega_3)-\frac{T^2}{D}(\Delta-\Delta\omega_3)(\Delta-\Delta\omega_2)\right] - \frac{M_2}{D_3}x_1^2T^2\left[4-\frac{T^2}{D_1}(2\Delta\omega_1+\Delta\omega_3)(\Delta\omega_1+\Delta\omega_2+\Delta\omega_3)-\frac{T^2}{D}(\Delta+\Delta\omega_1)(\Delta-\Delta\omega_2)\right], \quad \text{(A12)}$$

$$X_3 = \frac{1}{kD_5}\left\{x_1^2T^2\left[4-\frac{T^2}{D_1}(\Delta\omega_1+\Delta\omega_3+\Delta\omega_4)(\Delta\omega_1+\Delta\omega_2+\Delta\omega_3)-\frac{T^2}{D}(\Delta+\Delta\omega_4)(\Delta-\Delta\omega_2)\right] - \frac{M_3}{D_3}\left[x_1^2T^2\left[3-\frac{T^2}{D}(\Delta+\Delta\omega_1)(\Delta-\Delta\omega_2)\right]+x_4^2T^2\left[1-\frac{T^2}{D_1}(2\Delta\omega_1+\Delta\omega_3)(\Delta\omega_1+\Delta\omega_2+\Delta\omega_3)\right]\right]\right\}, \quad \text{(A13)}$$

$$D_4 = 1-\frac{M_1}{D_3D_5}\left[x_1^2T^2\left[3-\frac{T^2}{D}(\Delta+\Delta\omega_1)(\Delta-\Delta\omega_2)\right]+x_4^2T^2\left[1-\frac{T^2}{D_1}(2\Delta\omega_1+\Delta\omega_3)(\Delta\omega_1+\Delta\omega_2+\Delta\omega_3)\right]\right], \quad \text{(A14)}$$

$$D_5 = 1+\Delta\omega_2^2T^2+x_1^2T^2\left[5-\frac{T^2}{D}(\Delta-\Delta\omega_2)^2\right]+x_3^2T^2\left[1-\frac{T^2}{D_1}(\Delta\omega_1+\Delta\omega_2+\Delta\omega_3)^2\right]. \quad \text{(A15)}$$

Now the expression for P_{3i} is

$$P_{3i} = \frac{Z_1}{D_6} + \frac{Z_2}{D_6}P_{4i}, \quad \text{(A16)}$$

where

$$Z_1 = \frac{\epsilon_p}{\hbar}T|\mu_{bd}|^2\frac{\Delta N_{30}}{D_7} - \frac{\epsilon_p}{\hbar}T|\mu_{bd}|^2\frac{k}{D_3D_7}\Delta N_{10} \times x_3^2T^2\left[4-\frac{T^2}{D}(\Delta+\Delta\omega_1)(\Delta-\Delta\omega_3)-\frac{T^2}{D_1}(2\Delta\omega_1+\Delta\omega_3)(\Delta\omega_1+2\Delta\omega_3)\right] + X_1x_3^2T^2\frac{k}{D_7}\left[\left[3-\frac{T^2}{D}(\Delta-\Delta\omega_3)(\Delta-\Delta\omega_2)-\frac{T^2}{D_1}(\Delta\omega_1+2\Delta\omega_3)(\Delta\omega_1+\Delta\omega_2+\Delta\omega_3)\right] - \frac{M_1}{D_3}\left[4-\frac{T^2}{D}-(\Delta+\Delta\omega_1)(\Delta-\Delta\omega_3)-\frac{T^2}{D_1}(2\Delta\omega_1+\Delta\omega_3)(\Delta\omega_1+2\Delta\omega_3)\right]\right], \quad \text{(A17)}$$

$$Z_2=\frac{1}{D_7}\left\{-x_3^2T^2\left[3-\frac{T^2}{D}(\Delta+\Delta\omega_4)(\Delta-\Delta\omega_3)\right]-x_1^2T^2\left[1-\frac{T^2}{D_1}(\Delta\omega_1+\Delta\omega_3+\Delta\omega_4)(\Delta\omega_1+2\Delta\omega_3)\right]\right.$$
$$+\frac{M_3}{D_3}x_3^2T^2k\left[4-\frac{T^2}{D}(\Delta+\Delta\omega_1)(\Delta-\Delta\omega_3)-\frac{T^2}{D_1}(2\Delta\omega_1+\Delta\omega_3)(\Delta\omega_1+2\Delta\omega_3)\right]$$
$$+kX_3x_3^2T^2\left[\left[2-\frac{T^2}{D}(\Delta-\Delta\omega_3)(\Delta-\Delta\omega_2)-\frac{T^2}{D_1}(\Delta\omega_1+2\Delta\omega_3)(\Delta\omega_1+\Delta\omega_2+\Delta\omega_3)\right]\right.$$
$$\left.\left.-\frac{M_1}{D_3}\left[4-\frac{T^2}{D}(\Delta+\Delta\omega_1)(\Delta-\Delta\omega_3)-\frac{T^2}{D_1}(2\Delta\omega_1+\Delta\omega_3)(\Delta\omega_1+2\Delta\omega_3)\right]\right]\right\}, \tag{A18}$$

$$D_6=1-\frac{M_2}{D_3D_7}kx_3^2T^2\left[4-\frac{T^2}{D}(\Delta+\Delta\omega_1)(\Delta-\Delta\omega_3)-\frac{T^2}{D_1}(2\Delta\omega_1+\Delta\omega_3)(\Delta\omega_1+2\Delta\omega_3)\right]$$
$$-\frac{1}{D_7}kX_2x_3^2T^2\left[\left[2-\frac{T^2}{D}(\Delta-\Delta\omega_3)(\Delta-\Delta\omega_2)-\frac{T^2}{D_1}(\Delta\omega_1+2\Delta\omega_3)(\Delta\omega_1+\Delta\omega_2+\Delta\omega_3)\right]\right.$$
$$\left.-\frac{M_1}{D_3}\left[4-\frac{T^2}{D}(\Delta+\Delta\omega_1)(\Delta-\Delta\omega_3)-\frac{T^2}{D_1}(2\Delta\omega_1+\Delta\omega_3)(\Delta\omega_1+2\Delta\omega_3)\right]\right], \tag{A19}$$

$$D_7=1+\Delta\omega_3^2T^2+x_3^2T^2\left[5-\frac{T^2}{D}(\Delta-\Delta\omega_2)^2\right]+x_1^2T^2\left[1-\frac{T^2}{D_1}(\Delta\omega_1+\Delta\omega_2+\Delta\omega_3)^2\right]. \tag{A20}$$

Finally, the expression for P_{4i} is obtained as

$$P_{4i}=-\frac{\epsilon_sT_2}{\hbar D_8D_9}|\mu_{bd}|^2(\Delta N_{10}+\Delta N_{30}-\Delta N_{20})$$
$$-\frac{\epsilon_pT_2}{\hbar D_8}|\mu_{bd}|^2\frac{k\Delta N_{10}}{D_3D_9}x_3^2T^2\left[2-\frac{T^2}{D}(\Delta+\Delta\omega_1)(\Delta+\Delta\omega_4)-\frac{T^2}{D_1}(2\Delta\omega_1+\Delta\omega_3)(\Delta\omega_1+\Delta\omega_3+\Delta\omega_4)\right]$$
$$+\frac{X_1k}{D_4D_9D_8}x_3^2T^2\left[\left[4-\frac{T^2}{D}(\Delta-\Delta\omega_2)(\Delta+\Delta\omega_4)-\frac{T^2}{D_1}(\Delta\omega_1+\Delta\omega_2+\Delta\omega_3)(\Delta\omega_1+\Delta_3+\Delta\omega_4)\right]\right.$$
$$\left.-\frac{M_1}{D_3}\left[2-\frac{T^2}{D}(\Delta+\Delta\omega_1)(\Delta+\Delta\omega_4)-\frac{T^2}{D_1}(2\Delta\omega_1+\Delta\omega_3)(\Delta\omega_1+\Delta\omega_3+\Delta\omega_4)\right]\right]$$
$$+\frac{Z_1}{D_6D_8D_9}x_3^2T^2\left\{\left[-3+\frac{T^2}{D}(\Delta-\Delta\omega_3)(\Delta+\Delta\omega_4)+\frac{T^2}{D_1}k^2(\Delta\omega_1+2\Delta\omega_3)(\Delta\omega_1+\Delta\omega_3+\Delta\omega_4)\right]\right.$$
$$-\frac{M_2}{D_3}k\left[2-\frac{T^2}{D}(\Delta+\Delta\omega_1)(\Delta+\Delta\omega_4)-\frac{T^2}{D_1}(2\Delta\omega_1+\Delta\omega_3)(\Delta\omega_1+\Delta\omega_3+\Delta\omega_4)\right]$$
$$+\frac{x_2}{D_4}k\left[4-\frac{T^2}{D}(\Delta-\Delta\omega_2)(\Delta+\Delta\omega_4)-\frac{T^2}{D_1}(\Delta\omega_1+\Delta\omega_2+\Delta\omega_3)(\Delta\omega_1+\Delta\omega_3+\Delta\omega_4)\right.$$
$$-\frac{Z_1}{D_6D_3}\left[2-\frac{T^2}{D}(\Delta+\Delta\omega_1)(\Delta+\Delta\omega_4)\right.$$
$$\left.\left.\left.-\frac{T^2}{D_1}(2\Delta\omega_1+\Delta\omega_3)(\Delta\omega_1+\Delta\omega_3+\Delta\omega_4)\right]\right]\right\}, \tag{A21}$$

$$D_8=1-\frac{M_3}{D_3D_9}k\left[x_3^2T^2\left[2-\frac{T^2}{D}(\Delta+\Delta\omega_1)(\Delta+\Delta\omega_4)-\frac{T^2}{D_1}(2\Delta\omega_1+\Delta\omega_3)(\Delta\omega_1+2\Delta\omega_3)\right]\right]$$
$$-\frac{kx_3}{D_4D_9}\left[x_3^2T^2\left[4-\frac{T^2}{D}(\Delta+\Delta\omega_4)(\Delta-\Delta\omega_2)-\frac{T^2}{D_1}(\Delta\omega_1+\Delta\omega_2+\Delta\omega_3)(\Delta\omega_1+\Delta\omega_3+\Delta\omega_4)\right]\right.$$
$$\left.-\frac{M_1}{D_3}\left[2-\frac{T^2}{D}(\Delta+\Delta\omega_1)(\Delta+\Delta\omega_4)-\frac{T^2}{D_1}(2\Delta\omega_1+\Delta\omega_3)(\Delta\omega_1+\Delta\omega_3+\Delta\omega_4)\right]\right]$$
$$-\frac{Z_2}{D_6D_9}x_3^2T^2\left\{\left[-3-k^2+\frac{T^2}{D}(\Delta-\Delta\omega_3)(\Delta+\Delta\omega_4)+\frac{T^2}{D_1}k^2(\Delta\omega_1+2\Delta\omega_3)(\Delta\omega_1+\Delta\omega_3+\Delta\omega_4)\right]\right.$$
$$+\frac{M_2}{D_3}k\left[2-\frac{T^2}{D}(\Delta+\Delta\omega_1)(\Delta+\Delta\omega_4)-\frac{T^2}{D_1}(2\Delta\omega_1+\Delta\omega_3)(\Delta\omega_1+\Delta\omega_3+\Delta\omega_4)\right]$$
$$+\frac{X_2}{D_4}k\left[4-\frac{T^2}{D}(\Delta-\Delta\omega_2)(\Delta+\Delta\omega_4)-\frac{T^2}{D_1}(2\Delta\omega_1+\Delta\omega_3)(\Delta\omega_1+\Delta\omega_3+\Delta\omega_4)\right.$$
$$\left.\left.\left.-\frac{Z_1}{D_6D_3}k\left[2-\frac{T^2}{D}(\Delta+\Delta\omega_1)(\Delta+\Delta\omega_4)-\frac{T^2}{D_1}(2\Delta\omega_1+\Delta\omega_3)(\Delta\omega_1+\Delta\omega_3+\Delta\omega_4)\right]\right]\right\}, \tag{A22}$$

$$D_9=1+\Delta\omega_4^2T^2+x_3^2T^2\left[5-\frac{T^2}{D}(\Delta+\Delta\omega_4)^2\right]+x_1^2T^2\left[1-\frac{T^2}{D_1}(\Delta\omega_1+\Delta\omega_3+\Delta\omega_4)^2\right]. \tag{A23}$$

Hence the analytical expressions P_{1i}, P_{2i}, and P_{3i} may be found by using Eq. (A21). In these calculations we have assumed that $x_1=x_2$, $x_3=x_4$, $\mu_{ab}=\mu_{ac}$ and $\mu_{bd}=\mu_{cd}$.

---

*Author to whom correspondence should be addressed.

[1] A. Javan, Phys. Rev. **107**, 1579 (1957).
[2] H. R. Schlossberg and A. Javan, Phys. Rev. **150**, 267 (1966).
[3] M. S. Feld and A. Javan, Phys. Rev. Lett. **20**, 578 (1968).
[4] M. S. Feld and A. Javan, Phys. Rev. **177**, 540 (1968).
[5] B. J. Feldman and M. S. Feld, Phys. Rev. A **1**, 1375 (1970).
[6] T. W. Hänsch and P. Toschek, Z. Phys. **236**, 213 (1970).
[7] M. Takami, Jpn. J. Appl. Phys. **15**, 1063 (1976).
[8] M. Takami, Jpn. J. Appl. Phys. **15**, 1889 (1976).
[9] C. Feuillade and P. Berman, Phys. Rev. A **29**, 1236 (1984).
[10] S. Ghoshal and P. N. Ghosh, J. Chem. Phys. **83**, 4015 (1985).
[11] V. P. Chebotayev, in *High Resolution Laser Spectroscopy,* edited by K. Shimmoda (Wiley, New York, 1976), p. 201.
[12] S. Haroche and F. Hartmann, Phys. Rev. A **6**, 1280 (1972).
[13] J. Ekkers, A. Bauder, and Hs. H. Gunthard, J. Phys. E **8**, 819 (1970).
[14] R. H. Schwendeman, Ann. Rev. Phys. Chem. **29**, 537 (1978).
[15] W. H. Weber, Chem. Phys. Lett. **122**, 469 (1985).
[16] P. Glorleux, E. Arimondo, and T. Oka, J. Phys. Chem. **87**, 2133 (1983).
[17] T. Oka, Adv. At. Mol. Phys. **9**, 127 (1973).
[18] E. Arimondo, P. Gloriuex, and T. Oka, Phys. Rev. A **17**, 1375 (1978).
[19] J. Orr and T. Oka, Appl. Phys. **21**, 293 (1980).
[20] M. Dubs, D. Harradine, E. Schweitzer, and J. I. Steinfeld, J. Chem. Phys. **77**, 3824 (1982).
[21] C. Reiser, J. I. Steinfeld, and H. W. Galbraith, J. Chem. Phys. **74**, 2189 (1981).
[22] J. I. Steinfeld and C. C. Jenssen, in *Tunable Lasers and Applications,* edited by A. Mooradian, T. Jaeger, and P. Stokseth, (Springer, Berlin, 1976), p. 190.
[23] R. L. Shoemaker, in *Laser and Coherence Spectroscopy,* edited by J. I. Steinfeld (Plenum, New York, 1978), p. 197.
[24] T. G. Schmalz and W. H. Flygare, in *Laser and Coherence Spectroscopy* (Ref. [23]), p. 125.
[25] J. G. Baker, in *Modern Aspects of Microwave Spectroscopy,* edited by G. W. Chantry (Academic, New York, 1979), p. 65.
[26] W. Demtröder, *Laser Spectroscopy* (Springer-Verlag, Berlin, 1982).
[27] J. Brossel and F. Bitter, Phys. Rev. **86**, 308 (1952).
[28] P. Franken, Phys. Rev. **121**, 508 (1961).
[29] S. Haroche, in *High Resolution Laser Spectroscopy* (Ref. [11]), p. 253.
[30] N. Bloembergen and M. D. Levenson, in *High Resolution Laser Spectroscopy,* (Ref. [11]), p. 315.
[31] P. Jacquinot, in *High Resolution Laser Spectroscopy,* (Ref. [11]), p. 50.
[32] S. Ezekiel and R. Weiss, Phys. Rev. Lett. **20**, 91 (1968).
[33] J. C. McGurk, T. G. Schmalz, and W. H. Flygare, Adv. Chem. Phys. **25**, 1 (1974).
[34] S. Ghoshal and P. N. Ghosh, Opt. Commun. **73**, 455 (1989).
[35] P. N. Ghosh, Chem. Phys. Lett. **127**, 157 (1986).
[36] P. N. Ghosh and S. Mandal, Chem. Phys. Lett. **164**, 279

(1989).
[37] S. Mandal and P. N. Ghosh, Phys. Rev. A **45**, 4990 (1992).
[38] S. Mandal and P. N. Ghosh, Spectrochim. Acta **48A**, 1563 (1992).
[39] V. S. Letokhov and V. P. Chebotayev, *Nonlinear Laser Spectroscopy* (Springer-Verlag, Berlin, 1976).
[40] J. L. Hall and C. Borde, Phys. Rev. Lett. **30**, 1101 (1973).
[41] T. W. Hänsch, M. H. Nayfeh, S. A. Lee, S. M. Curry, and I. S. Shahin, Phys. Rev. Lett. **32**, 1336 (1974).
[42] S. Stenholm, *Foundations of Laser Spectroscopy* (Wiley, New York, 1983).
[43] M. Göpert-Mayer, Ann. Phys. **9**, 273 (1931).
[44] G. Grynberg, B. Cagnac, and F. C. Biraben, in *Coherent Nonlinear Optics,* edited by M. S. Feld and V. S. Letokhov, (Springer, Berlin, 1980), p. 111.
[45] Y. Makdisi and K. S. Bhatia, Can. J. Phys. **68**, 1464 (1990).
[46] W. M. Huo, K. D. Rinnen, and R. N. Zare, J. Chem. Phys. **95**, 205 (1991).
[47] J. M. Gilligan and E. E. Eyler, Phys. Rev. A **43**, 6406 (1991).
[48] M. Mizushima, Jpn. J. Appl. Phys. Lett. **29**, L2121 (1990).
[49] G. Adam, J. Seke, and O. Hittmair, Phys. Rev. A **42**, 5522 (1990).
[50] W. H. Weber and R. W. Terhune, J. Chem. Phys. **78**, 6437 (1983).